



The publisher regrets that information was missing from the original article, "An Evaporation-Based Disposable Micropump Concept for Continuous Monitoring Applications" by Effenhauser, Harttig and Kramer, which appeared in *Biomedical Microdevices 4:1*. The article is printed in its entirety below.

An Evaporation-Based Disposable Micropump Concept for Continuous Monitoring Applications

Carlo S. Effenhauser, Herbert Harttig,
and Peter Krämer*

*Roche Diagnostics GmbH, Roche Diabetes Care, New Technologies
DD-T, Sandhoferstr. 116, D-68305 Mannheim, Germany
E-mail: carlo.effenhauser@roche.com*

Abstract. An inexpensive and simple pumping principle is described that is capable of delivering both small and constant flow rates (10–1,000 nl/min) over a longer period of time (days to weeks). The concept is based on controlled evaporation of a liquid through a membrane into a gas space containing a sorption agent. As long as the sorption agent keeps the vapor pressure in the gas phase below saturation, fluid evaporated from the membrane is replaced by capillary forces inducing flow from a reservoir. In a feasibility study, a total volume of 300 μ l of Ringer's solution has been continuously pumped over a period of six days, resulting in a constant average flow rate of 35 nl/min (590 pl/s). The maximum liquid volume transported is limited by sorption capacity and amount of the sorption agent. Low fabrication costs, high reliability (no moving parts), the suitability for integration into planar system architectures and the lack of a special external energy source besides an environment of regulated temperature are important features of the concept, in particular with regard to its potential application in continuous patient monitoring. Truly continuous flow can be achieved in contrast to many other pump mechanisms leading to discontinuous, pulse-type flow. A challenge for a broader range of applications is the inherent temperature dependence of the flow rate. In its current version, the pump can only be used in a suction-mode.

Key Words. microfluidics, micropumps, continuous monitoring

Introduction

Currently, many attempts are underway to develop inexpensive, reliable, and miniaturized means for the precise control of small amounts of liquids in microcavities (Shoji et al., 1998; Elwenspoek et al., 1994; Wego and Pagel, 2001; Nguyen and Huang, 2001; Andersson et al., 2001; Unger et al., 2000). Electrokinetic fluid handling is one particularly appealing method (Effenhauser, 1998 and Kutter, 2000), since it requires no moving parts and allows for

highly parallel system architectures. The inherent drawbacks of electrokinetic fluid manipulation such as electrode gas formation, pH and ionic strength dependence, however, will not be tolerable in a considerable range of biomedical applications. These limitations and the lack of an alternative, universal fluid control system require successful product development to rely on finding particularly suited concepts for the specific application of interest. A novel fluid propulsion concept developed for microdialysis-based continuous monitoring of glucose level in diabetic patients (Vering et al., 1998; Kaptein et al., 1998; Sternberg et al., 1995; Perdomo et al., 2000; Lutgers et al., 2000; Hulleger et al., 2000; Tamura et al., 2000), is presented here to underline the importance of finding tailor-made solutions. Subsequently, the application shall be outlined briefly to present the requirements on the flow control system.

A very promising approach towards continuous glucose monitoring is currently based on the continuous diffusion of glucose across a dialysis membrane of suitable molecular weight cut-off. A dialysis solution is pumped in a constant fashion through a microdialysis catheter, followed by electrochemical detection of glucose in the dialysate downstream of the catheter. The catheter contains the dialysis membrane and is inserted into the patient's body. Given a sufficiently long residence time of the dialysis solution within the membrane exchange area, the steady state concentration in the dialysate will approach the local analyte concentration in the tissue (high recovery time). The minimum recovery needed thus imposes an upper limit on the linear flow velocity for a given membrane exchange area. The maximum membrane exchange

*Corresponding author.

area is predominantly limited by the catheter size, which in turn is determined by the minimum invasive nature of the system. As a consequence, flow rates are typically in the order of 0.1–1 $\mu\text{L}/\text{min}$. The catheter is usually used over a couple of days up to several weeks. Correspondingly, the flow system has to provide a constant flow rate over the identical time period.

The low flow rates required above and the characteristic times of operation of the system result in very low consumption of dialysis solution. For example, only 1 mL of solution is consumed when a flow rate of 100 nL/min is maintained over one week. Thus an autonomous microdialysis chip becomes feasible, where all the fluid handling is integrated into a disposable device. Böhm et al. (2000) and Bergveld (2000), have demonstrated a step towards integration, where catheter adapters, means for dosing of calibration solutions, and chemical sensors have been integrated into one device. However, the highly desirable integration of a low-cost micropump into the disposable device itself is currently still missing. The demands on a suitable micropump are:

1. Constant delivery of small flow rates.
2. Minimization of pump size and weight.
3. Minimization of energy consumption.
4. Simplicity and reliability of construction and operation.
5. Minimization of manufacturing costs enabling disposability.
6. Compatibility with planar system architectures (microtechnology).
7. Feasibility of pump sterilization.

An impressive arsenal of pumps, based on silicon and polymer micromachining, has been described (Shoji, 1998; Elwenspoek et al., 1994; Wego and Pagel, 2001; Nguyen and Huang, 2001; Andersson et al., 2001). However, thorough investigation reveals that the constant delivery of small flow rates cannot be met by any of the pumps reported without significant further development, in particular under the side condition of a very inexpensive pump manufacturing process enabling disposability. Alternatively, we present here a novel concept which meets all requirements.

Liquid propulsion from a reservoir is affected by controlled evaporation of liquid through a membrane into a gas chamber located above the membrane. The vapor pressure in the gas chamber is kept below saturation and controlled by a suitable adsorption agent added to the gas chamber. Evaporated liquid is continuously replaced by liquid flow through the microfluidic system of interest, e.g., the microdialysis catheter. Sufficient amounts of adsorbents added allow for a constant flow rate over the time of operation. The pump principle presented bears some resemblance to the xylem transport system in trees (Taiz and Zeiger, 1998).

Experimental Methods

The flow control system, depicted in Figure 1, consists of a pump body, a liquid exchange device, a liquid reservoir and capillaries, which connect all modules. A schematic representation of the pump body, depicted in Figure 2, features a flow channel and a gas chamber, which is filled with a desiccant (molecular sieve MS 518, Grace Davison, Baltimore, Maryland, USA, sorption capacity 17% w/w). The gas chamber was closed with a Plexiglas lid. The external dimensions of the pump body were chosen to allow convenient experimentation with outer dimensions of about $3 \times 2 \times 2$ cm. The cylindrical flow channel was 1 mm in diameter and 20 mm in length. The edges of a circular polysulfone membrane (Memtec BTS 65) were mounted concentrically on top of the flow channel outlet. This strongly hydrophilic membrane is asymmetric with pores in the range of some 10 μm on the coarse pore side and an average pore size of 0.1 μm on the fine pore side. The coarse pore side of the membrane faced the liquid. Leaking of liquid by lateral flow was prevented by adhesively sealing the edges of the membrane. A hole punched in the adhesive tape (1 mm) defines the active area of the membrane from which the liquid can evaporate. The desiccant was placed on in a small plastic vessel to avoid direct contact of membrane and desiccant.

The liquid exchange device is illustrated in Figure 3. A Plexiglas block consists of 8 cylindrical reservoirs (diameter: 4 mm, length: 10 mm, volume 125 μL each), which is sealed with a Plexiglas lid. The reservoirs were interconnected by short capillaries (length: 3 mm, I.D.: 100 μm). The capillaries connecting the pump body and the liquid exchange device was 100 μm in diameter and 10 and 30 mm in length, respectively. Ringer's saline (Fresenius GmbH, D61346 Bad Homburg, Germany), colored with Brilliant Blue was used for visualization purposes.

The fluidic system was filled with degassed water by means of a peristaltic pump prior to pumping Ringer solution from the liquid reservoir to the liquid exchange device. Once the membrane was completely soaked with the transport liquid, capillary 1 (Figure 1) was placed in the Ringer solution reservoir and the lid of the pump housing was fixed on top of the membrane. Pumping action started after evaporation of remaining excess water from the top of the membrane after about 30 minutes to 1 h, often accompanied by erratic fluctuations of the flow rate before stable flow was obtained.

The flow rate was determined gravimetrically by measuring the weight of liquid reservoir, which was filled with approx. 4 mL of Ringer solution and exposed to ambient pressure. A drop of vacuum pump silicone oil

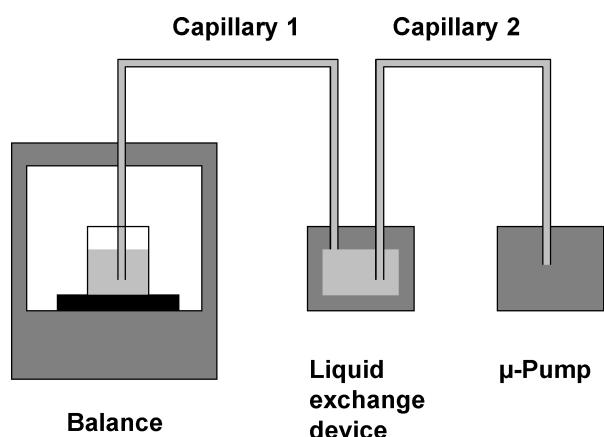


Fig. 1. Schematic representation of the set-up of the flow control system.

(Edwards, Ultra Grade 19) was placed onto the liquid meniscus to prevent evaporation. All experiments were performed in a room of regulated temperature (about 30 °C), in all cases a Mettler Toledo AT 261 balance was used. The least significant digit of the balance of 10 μg corresponds to a volume of 10 nanoliter (nl). The weight of the reservoir was recorded every 5 minutes and the net flow rate was determined from the difference of successive data points. All modules except the liquid reservoir were thermally controlled by placing them into a thermostated bath. Ambient air temperature was recorded next to the pump with a data logger system with integrated temperature/humidity sensors (Testostor 175, Testo GmbH, Germany). Data were acquired with a Meilhaus 3000 multipurpose data acquisition board, operated under HP VEE software.

The fluidic system was filled with degassed water by means of a peristaltic pump prior to pumping Ringer solution from the liquid reservoir to the liquid exchange device. Once the membrane was completely soaked with the transport liquid, capillary 1 (Figure 1) was placed in the Ringer solution reservoir and the lid of the pump housing was fixed on top of the membrane. Pumping action started after evaporation of remaining excess water from the top of the membrane after about 30 minutes to 1 hour, often accompanied by erratic fluctuations of the flow rate before stable flow was obtained.

The flow rate was determined gravimetrically by measuring the weight of liquid reservoir, which was filled with approx. 4 mL of Ringer solution and exposed to ambient pressure. A drop of vacuum pump silicone oil (Edwards, Ultra Grade 19) was placed onto the liquid meniscus to prevent evaporation. All experiments were performed in a room of regulated temperature (about 30 °C), in all cases a Mettler Toledo AT 261 balance was used. The least significant digit of the balance of 10 μg corresponds to a volume of 10 nanoliter (nl). The weight

of the reservoir was recorded every 5 minutes and the net flow rate was determined from the difference of successive data points. All modules except the liquid reservoir were thermally controlled by placing them into a thermostated bath. Ambient air temperature was recorded next to the pump with a data logger system with integrated temperature/humidity sensors (Testostor 175, Testo GmbH, Germany). Data were acquired with a Meilhaus 3000 multipurpose data acquisition board, operated under HP VEE software.

Results and Discussion

Ideally, a pump should be capable of pumping any kind of solution including dissolved components (ionic or non-ionic) and particulates. In an evaporation-based micropump, however, all components of the liquid that cannot be evaporated will be concentrated and precipitated at the site of evaporation. As a result, the evaporation rate will gradually change and cannot be held at a constant rate for a longer period of time. We studied this effect in an initial attempt to pump Ringer's solution in a set-up similar to the one shown in Figure 2, the difference being that the vessel of Ringer's solution was directly connected to the pump body. The resulting formation of a salt crust at the membrane is depicted in Figure 4. Constant flow rates over several days could not be reached (data not shown). As a solution to this problem, and to the more general problem that for some liquids to be pumped suitable sorption agents might not exist, we devised a so-called liquid exchange device. The purpose of this device is to ensure that during the operation time of the pump, the membrane will only come into contact with an appropriate transport liquid (e.g., deionized water), thus preventing accumulation of any particulate, salt precipitation, etc. in the membrane. In order to demonstrate the function of the liquid exchange device Ringer's solution colored with brilliant

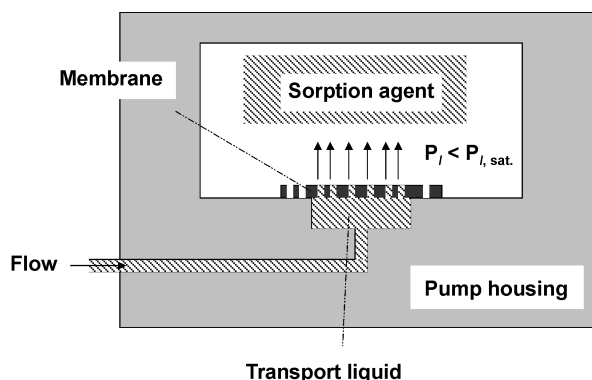


Fig. 2. Principal set-up of a membrane evaporation-based pump.

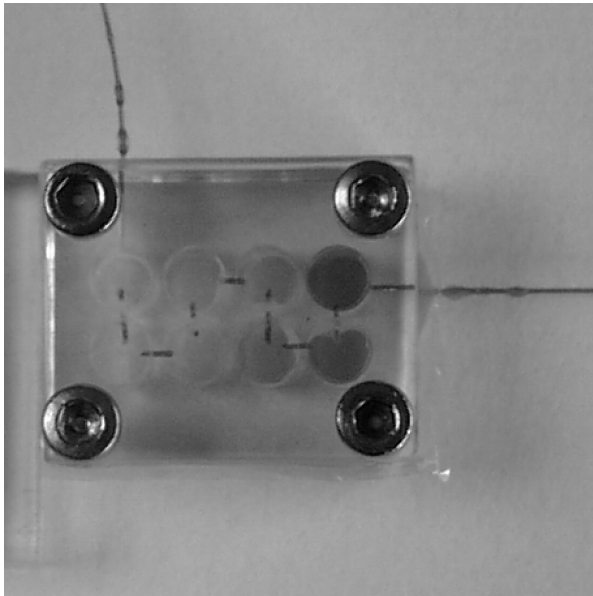


Fig. 3. Liquid exchange device that stores the actual transport liquid. The photograph shows the distribution of a colored Ringer's solution after 144 hours of pumping action.

blue was transported for 144 hours. The resulting distribution of the dye in the compartments after six days is shown in Figure 3. As can be seen, the Ringer's solution (coming from the right) displaced most of the original transport fluid (deionized water) through the capillary on the top, however, even after one week the solution was prevented from direct contact with the pump membrane thanks to a gradual dilution process over a cascade of containers. A drawback of this concept is the additional volume that is required and a more complex manufacturing process (filling procedure, adequate storage of the assembled pump, initialization procedure).

Incorporation of this liquid exchange device into the experimental set-up (Figure 1) allowed us to pump Ringer's solution with a membrane evaporation based pumping mechanism. Figure 5 shows a typical result of flow rate of as a function of time. After 140 hours, when the flow rate started to decline, a total volume of 300 μl of water was pumped through the device at an average flow rate of 35.5 nl/min (590 pl/s). The upper limit as calculated by the capacity of the desiccant corresponds to 340 μl (2 g desiccant, 17% w/w), thus the decrease of the flow rate after around six days of operation corresponds well with the capacity of the sorption agent. The temperature in the vicinity of the pump was regulated at $30 \pm 0.5^\circ\text{C}$ and is also shown in Figure 4. Basically, the evaporation process from the membrane surface will take place as long as there exists a spatial gradient of vapor pressure in the gas phase above the membrane. Evaporation will cease when this gradient

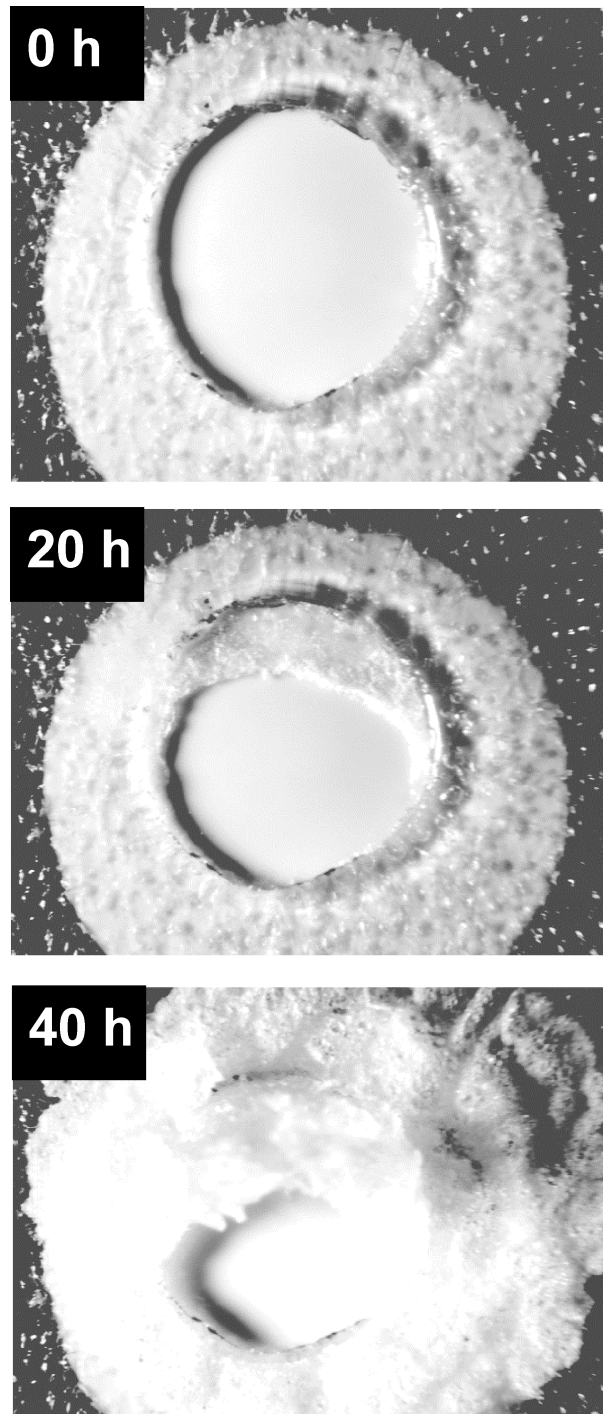


Fig. 4. Photographs of the evaporation membrane, showing the formation of a salt crust after 0, 20, and 40 hours of continuous evaporation of Ringer's solution through the membrane.

has vanished and the vapor pressure in the gas phase has assumed the saturation vapor pressure at the given temperature. Consequentially, constant flow rates require the temperature of the pump to be held at a constant level. In continuous monitoring applications, where the

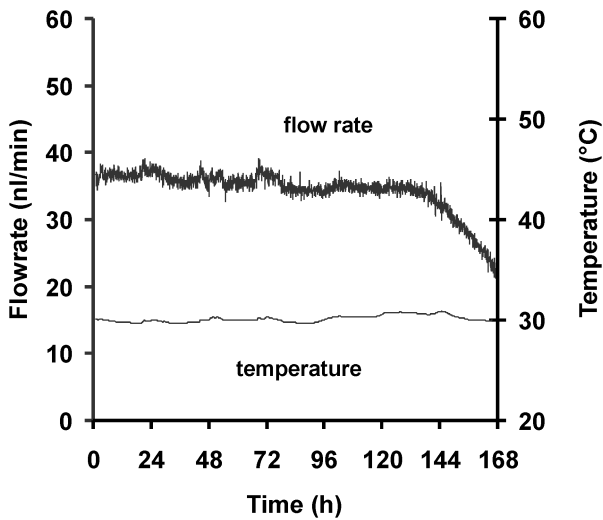


Fig. 5. Flow rate of the pump as a function of time. (BGS 65 membrane, diameter 1 mm, sorption agent: 2 g MS 518). Also shown is the temperature in the vicinity of the pump.

pump is fixed at or close to the skin surface of the patient, this condition can be fulfilled to an acceptable level and the patient will act as a thermostat.

The impact of temperature on the flow rate should be expected to be rather complex, as it is correlated to the result of the individual temperature dependence of a wide variety of intrinsic factors, such as viscosity, surface tension, enthalpy of evaporation of the transported (evaporated) liquid, and the sorption rate and capacity of the sorption agent, to name just a few. In addition to these intrinsic factors, extrinsic contributions come into play such as the temperature dependence of the pressure of the enclosed gas volume and the thermal expansion of the membrane. We chose to determine the impact of temperature variation on the flow rate experimentally. A typical result is shown in Figure 6. During periods when the temperature was held at a constant level, the flow rate was also found to be fairly constant, and generally decreased with decreasing temperature and vice versa. The relative temperature dependence of the flow rate was found to be about 3–4% per K.

However, apart from this expected trend, temperature changes were also accompanied by a more complex response, the reason of which we trace back to the thermal expansion of the enclosed gas volume. Due to the fact that the thermal diffusivity of gases is about two orders of magnitude higher compared to most liquids and polymers (air: $2.20 \cdot 10^{-5} \text{ m}^2 \text{ s}^{-1}$, water: $1.46 \cdot 10^{-7} \text{ m}^2 \text{ s}^{-1}$, Plexiglas: $\approx 1.1 \cdot 10^{-7} \text{ m}^2 \text{ s}^{-1}$, resp., at 298 K), the gas will respond to temperature variations in the environment on a faster time scale. In the case of decreasing temperature, the resulting fast pressure drop in the gas container (rigid walls) will exert

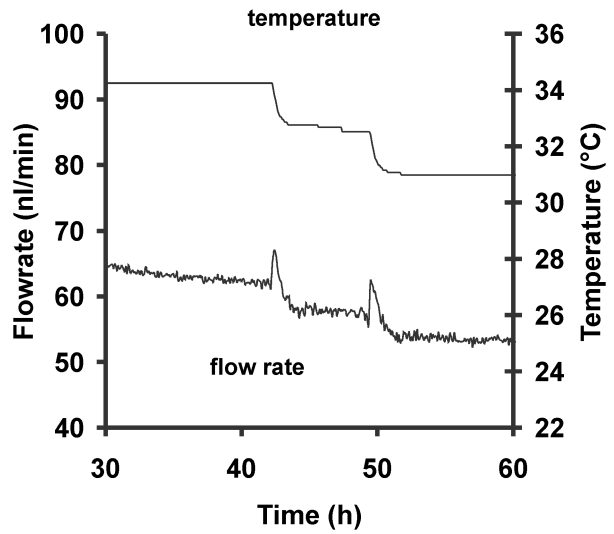


Fig. 6. Temperature dependence of the flow rate. The whole pump was emerged into the bath of a thermostat. For a discussion of the features, see text.

a force pulling the membrane away from the liquid. This bending motion will be accompanied with an additional transient flow in the original flow direction, the maximum of which corresponds to the highest bending rate of the membrane. When the membrane bending has finally come to an end, influenced also by the mechanical properties of the membrane, the induced additional flow will cease and a new steady state flow will be reached at a lower level corresponding to the lower temperature (smaller evaporation rate). This interpretation is corroborated by the opposite behavior found with increasing temperature (Figure 7). In this case, the membrane will

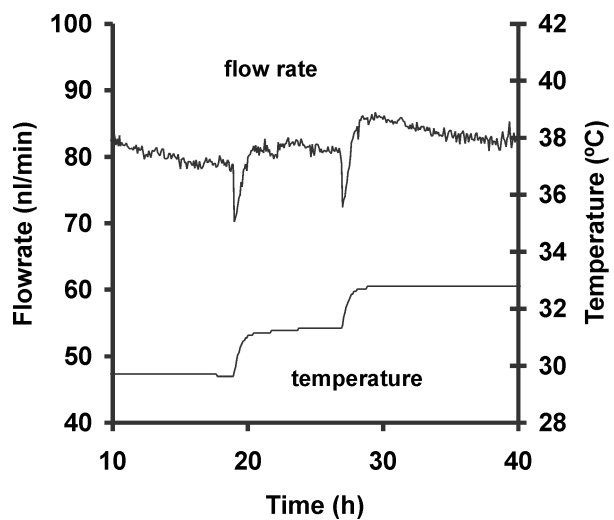


Fig. 7. Temperature dependence of the flow rate. The whole pump was emerged into the bath of a thermostat. For a discussion of the features, see text.

be pushed towards the liquid side (lower pressure side), and a transient flow pulse of decreased flow rate will result.

Integration of the flow rate “dips” and “peaks”, respectively, in Figures 6 and 7 over time allows a rough estimation of the maximum displacement of the membrane center due to bending. The corresponding volume of about 220 nl per “dip” (positive ΔT) and 150 nl per “peak” (negative ΔT), respectively, corresponds to a maximum displacement of the center of the membrane in the order of a 60 and 40 μm , respectively, based on the model of a spherically deformed membrane. This asymmetry can be made plausible due to the fixation of the membrane on the Plexiglas body by means of adhesive tape, as pulling or pushing forces acting on the membrane will lead to different bending. Mechanical support of the membrane on either side should alleviate or even avoid this kind of behavior.

Even if the membrane were completely rigid, the pressure difference would still to impact the pump rate in the following way. In a hydrophilic membrane, surface forces will lead to a complete wetting and filling of the membrane with liquid. If the pressure on the gas side is raised, or equivalently the pressure on the liquid side is lowered, liquid will be purged from the largest pores of the membrane corresponding to Laplace's law $\Delta p = 2 \sigma \cos \theta / r$ (Probstein, 1994), where Δp denotes the pressure difference across the gas/liquid boundary, σ the surface tension of the liquid, θ the contact angle, and r the pore radius. If this takes place, gas will be flowing through the membrane until the pressure gradient has vanished. The resulting gas bubble will eventually occlude the membrane and the pumping action will cease. If the pressure gradient is applied the other way round and exceeds a threshold (higher pressure on the liquid side), liquid will be forced out of the membrane and the pump will be flooded. In this case, pumping action will also cease, as liquid will evaporate simply from the bulk phase above the membrane and capillary action will not compensate for the liquid loss until all excess water has been evaporated. Thus the ideal membrane would be hydrophilic with very small pores of uniform size, so that the pumping action becomes less dependent on temperature and/or pressure gradients. Using homogenous dialysis membranes, such as the cellulose-based Cuprophan[®] or the polycarbonate-based Gambrane[®], should avoid some of the drawbacks of microporous membranes, although some run-in time might be necessary caused by membrane swelling. Suitable membranes could also be fabricated by microfabrication means as described, e.g., Desai et al. (1999).

Conclusions

An inexpensive and simple pumping principle has been demonstrated for achieving both small and constant flow rates (10–1,000 nl/min) over a longer period of time (days to weeks). A total volume of 300 μl of Ringer's solution has been continuously pumped over a period of six days, resulting in an constant average flow rate of 35 nl/min (590 pl/s). Apart from the low fabrication costs, an important feature of the concept is the lack of an external energy source in a continuous patient monitoring application, as the energy will be provided by the body (skin surface) of the patient. Other advantages include its reliability (no moving parts), its suitability for integration into planar system architectures fabricated, e.g., in polymer materials by hot embossing, injection molding, or by a laser ablation process. A challenge can be found in the inherent temperature dependence of the flow rate of 3–4% per Kelvin, thus requiring a thermostated environment for highly constant flow. In its current version, the pump can only be used in a suction-mode. The current construction and fabrication principle of the pump, though not microtechnology-based in the classical sense, exhibits a significant potential for further miniaturisation and integration into many complex microfluidic systems.

Acknowledgments

The authors are grateful to Dr. Gregor Ocvirk, Roche Diagnostics Mannheim, for critical reading of the manuscript and numerous helpful suggestions and comments, and to Dr. Michael Hein, Roche Diagnostics Mannheim, for his support of the project.

References

- H. Andersson, W. Vander Wijngaart, P. Nilsson, P. Enoksson, and G. Stemme, *Sensors & Actuators B* **72**, 259–265 (2001).
- P. Bergveld, *Biomedical Microdevices* **2**, 185–195 (2000).
- S. Böhm, W. Olthuis, and P. Bergveld, *Biomedical Microdevices* **1**, 121–130 (2000).
- T.A. Desai, D.J. Hansford, L. Kulinsky, A.H. Nashat, G. Rasi, J. Tu, Y. Wang, M. Ahang, and M. Ferrari, *Biomedical Microdevices* **2**, 11–40 (1999).
- C.S. Effenhauser, *Topics in Current Chemistry* **194**, 51–82 (1998).
- M. Elwenspoek, T.S.J. Lammerink, R. Miyake, and J.H.J. Fluitman, *Journal of Micromechanics Micro-engineering* **4**, 227–245 (1994).
- L.M. Hulleger, H.L. Lutgers, R.P.F. Dullaart, W.J. Sluiter, K.J. Wientjes, A.J.M. Schoonen, and K. Hoogenberg, *The Netherlands Journal of Medicine* **57**, 13–19 (2000).
- W.A. Kaptein, J.C. Zwaagstra, K. Venema, and J. Korf, *Analytical Chemistry* **70**, 4696–4700 (1998).
- J.P. Kutter, *Trends in Analytical Chemistry* **19**, 352–363 (2000).

- H.L. Lutgers, L.M. Hullegie, K. Hoogenberg, W.J. Sluiter, R.P.F. Dullaart, K.J. Wientjes, and A.J.M. Schoonen, *The Netherlands Journal of Medicine* **57**, 7–12 (2000).
- N.-T. Nguyen and X. Huang, *Sensors & Actuators A* **88**, 104–111 (2001).
- J. Perdomo, H. Hinkers, C. Sundermeier, W. Seifert, O. Martinez Morell, and M. Knoll, *Biosensors & Bioelectronics* **15**, 515–522 (2000).
- R.F. Probstein, ‘‘Physicochemical Hydrodynamics’’, 2nd edn, Wiley, New York, 1994.
- S. Shoji, *Topics in Current Chemistry* **194**, 163–188 (1998).
- F. Sternberg, C. Meyerhoff, F. Mennel, F. Bischoff, and E.F. Pfeiffer, *Diabetes Care* **18**, 1266–1269 (1995).
- L. Taiz and E. Zeiger, ‘‘Plant Physiology’’, 2nd edn, Whitaker, 1998.
- T. Tamura, K. Koseki, T. Sumino, M. Ogawa, T. Togawa, and K. Tsuchiya, *Frontiers in Medical and Biological Engineering* **10**, 147–156 (2000).
- M.A. Unger, H.-P. Chou, T. Thorsen, A. Scherer, and S.R. Quake, *Science* **288**, 113–116 (2000).
- T. Vering, S. Adam, H. Drewer, C. Dumschat, R. Steinkuhl, A. Schulee, E.M. Siegel, and M. Knoll, *Analyst* **123**, 1605–1609 (1998).
- A. Wego and L. Pagel, *Sensors & Actuators A* **88**, 220–226 (2001).